Measurement 170 (2021) 108706

Contents lists available at ScienceDirect

Measurement

journal homepage: www.elsevier.com/locate/measurement

Sensing performance improvement of resonating sensors based on knotting micro/nanofibers: A review

Hongtao Dang [a], Mingshu Chen [a], Jin Li [b,c,*], Wei Liu [d]

[a] Shaanxi Engineering Research Center of Controllable Neutron Sources, School of Science, Xijing University, Xi'an 710123, China
[b] State Key Laboratory of Applied Optics, Changchun Institute of Optics, Fine Mechanics and Physics, Chinese Academy of Sciences, Changchun 130033, China
[c] College of Information Science and Engineering, Northeastern University, Shenyang 110819, China
[d] Xian Tellhow IR-tech. Co., Ltd, Xi'an 710119, China

ARTICLE INFO

Keywords:
Microfiber sensor
Knot resonator
Miniature sensor
Integrated optics

ABSTRACT

Compared with traditional optical fibers, optical micro/nanofibers can support the large proportion of evanescent fields, high efficiency optical coupling, low bending loss and high sensitivity, which have paved their way to all-optical transmission, environmental monitoring and life sciences. Because of the high quality factor, simple fabrication process and low cost, the microfiber knot resonator was used to explore some novel micro/nano-photonic devices, for example, micro-lasers and sensors. Where, the sensing performance was improved by elaborating the fiber surface or packaging the whole structures with the sensitive materials, enabling the sensors for determining the temperature, humidity, radiation intensity, current, gas concentration, etc. In this review, the microfiber knot resonators reported in the last decade have been reviewed, compared and analyzed. The future research has been prospected finally.

1. Introduction

The diameter of micro/nanofiber (MNF) is generally ranged during 100 nm to 10 μm. After being launched into the MNF, the light will mostly transfer along its surface in the form of evanescent wave [1,2]. It is extremely sensitive to the external environment for developing compact and sensitive micro-sensors with high performance attributed to the introduction of different structures and sensitive materials [3–6]. The evanescent field can be retrained and transmitted along the out surface of the MNF with low optical loss, resulting in the high-efficiency light coupling between MNFs [7]. Therefore, the resonators based on MNFs are realized in three typical structures, including the loop, knot and coil forms. They have been further used for exploring optical modulator, filter, laser with high quality (Q) factor, and the sensing system with high precision [8–10]. For the resonator structures mentioned above, the light beam will be separated at the coupling region of MNFs, one part will transmit circle along the ring section and another beam will go through the direct section. These two parts interfere to each other and excite a resonant peak with the special wavelength or intensity, depending on the diameter or surrounding environment of MNFs and the ring length of the resonator structures [11]. The calibration techniques were different depending on the morphology and structure of MNFs. The transmission/reflection intensity of single-cone and doped-MNF changes obviously, and the sensing performance is calibrated by the optical power [12]; the transmission spectra of double-cone and composite-MNF structures show the interference of multipath light, and the signal needs to be demodulated through the phase change of the resonance wavelength [13].

MNF loop resonator (MLR) is prepared through bending a MNF into ring without immobilization, where the structure is maintained by the van der Waals force between the MNFs and easily affected or even destroyed by the small fluctuations from the environment, leading to its shift of the coupling condition and the serious decreasing of the sensing performance [14]. MNF coil resonator (MCR) is obtained by winding multi-loops MNF on the dielectric rods with low refractive index to limit the light loss [15]. In addition to its complex structure and preparation process, the relatively high Q factor has been demonstrated [16]. MNF knot resonator (MKR) is more stable than MLR and simpler than MCR [17]. This structure is not easily affected by the external environment. The ring length is changed to flexible manipulate the output spectral characteristics such as free spectral range and output intensity. In 2003, Tong [18] firstly proposed MNF concept and fabricated a MKR with a

* Corresponding author at: State Key Laboratory of Applied Optics, Changchun Institute of Optics, Fine Mechanics and Physics, Chinese Academy of Sciences, Changchun 130033, China.
E-mail address: lijin@ise.neu.edu.cn (J. Li).

https://doi.org/10.1016/j.measurement.2020.108706
Received 7 September 2020; Received in revised form 1 November 2020; Accepted 5 November 2020
Available online 10 November 2020

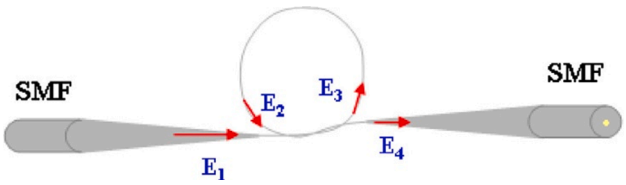

Fig. 1. Schematic diagram of light transmission in MKR [20].

diameter of 150 μm. The Q factor of 1500 was measured preliminarily at 1500 nm, and the mechanism of light transmission in MKR was analyzed. In recent years, MKR based sensors have been widely concerned and widely used in many fields, such as physical parameter measurement, chemical reaction monitoring, and bio-molecular analysis [19]. In this paper, the latest research on MKR sensors for measuring temperature, humidity, refractive index, current and other parameters were reviewed.

2. Working mechanism of MKR

Due to the high efficiency self-coupling between MNFs in the overlapping region of MKR, the very low loss and high Q factor are obtained. The corresponding mechanism can be explained by combining the directional coupler theory [20,21] with the waveguide ring resonator theory [22–24]. The MKR coupling model is shown in Fig. 1. It is assumed that the MKR has the excellent uniformity (in its diameter), surface smoothness, and negligible propagation loss [25]. The bending loss caused by the small diameter of the optical fiber can be ignored.

The transmission matrix of MKR is expressed as [20]:

$$\begin{bmatrix} E_3 \\ E_4 \end{bmatrix} = \sqrt{1-r_0}\begin{bmatrix} \sqrt{1-k} & j\sqrt{k} \\ j\sqrt{k} & \sqrt{1-k} \end{bmatrix}\begin{bmatrix} E_1 \\ E_2 \end{bmatrix} \tag{1}$$

where, E_3 and E_4 refer to the transmission intensities, E_1, E_2 refer to the incident optical signals, r_0 and K stand for the loss and coupling factor of MKR, respectively.

When E_1 is launched in the MKR with a perimeter of L, the light beam is separated to E_3 and E_4 after the coupling region. The light beam E_3 will transmit circle and enter into the coupling region again to produce the interference spectrum. Based on the optical field transmission matrix in Eq. (1), the light intensities at different ports are calculated as [21–23]:

$$E_2 = E_3 \exp(j\beta L) \tag{2}$$

$$E_3 = \frac{\sqrt{(1-r_0)(1-k)}E_1}{1-j\sqrt{k(1-r_0)}exp(j\beta L)} \tag{3}$$

$$E_4 = \left(j\sqrt{k(1-r_0)} + \frac{(1-k)(1-r_0)exp(j\beta L)}{1-j\sqrt{k(1-r_0)}\,exp(j\beta L)}\right)E_1 \tag{4}$$

where β represents the propagation constant [23,24]:

$$\beta = \frac{2\pi}{\lambda} + \frac{\gamma^2\lambda}{4\pi} \tag{5}$$

$$\gamma = \frac{2.246}{d}exp\left[\frac{n_{12}+n_{22}}{8n_{22}} - \frac{n_{12}+n_{22}}{n_{22}(n_{12}-n_{22})}\frac{\lambda^2}{(\pi d)^2}\right] \tag{6}$$

d refers to the diameter of the microfiber; n_1 and n_2 are the refractive index of the MNF and external environment, respectively. The incident optical signal E_1 is assumed as a constant 1; the transmission coefficient can be expressed by [24]:

$$T = \frac{|E_4|^2}{|E_1|^2} = \left|j\sqrt{k(1-r_0)} + \frac{(1-k)(1-r_0)exp(j\beta L)}{1-j\sqrt{k(1-r_0)}\,exp(j\beta L)}\right|^2 \tag{7}$$

The impact factors for the light intensity of MKR include: d-the diameter of the MNF; λ-the working wavelength; L-a perimeter of resonant ring; r_0-light loss coefficient. MKR acts as a high-precision sensor by bridging above optical parameters with the external parameters, covering temperature, humidity, refractive index, current and others.

It is known from Eq. (6) that the propagation constant depends on the transmission wavelength, the diameter of optical fiber and the refractive index of fiber core. The output spectrum can be characterized by four parameters: free spectrum range, fringe fineness, quality factor, and extinction ratio. The output spectra of MKR are affected by the circumference of the micro-ring, the coupling coefficient and the transmission loss coefficient. The coupling coefficient/efficiency is related to the strength of evanescent field on the surface of MNF, the distance between the two microfibers and the length of the coupling region. The circumference of the micro-ring can be controlled in the experimental process, and the transmission loss coefficient is determined by the MNF material.

3. MKR sensors

3.1. Temperature sensing applications

Silica MKR can be prepared from the normal single mode optical fiber. It generates the gallery mode resonance and serves as the sensing probe without package. In 2013, Li and Ding [26] theoretically and experimentally studied the relationship between the thermal effect of MKR and its structural parameters. It is concluded that MKR's thermal characteristics seriously depend on the diameter of optical fiber, as well as the environment's optical parameters (sensitive materials or analyte). By balancing the three parameters, the temperature performance has been optimized in several works. In 2014, Yang [27] et al. studied the relationship among seawater temperature sensitivity, optical fiber diameter and detection wavelength. They found that a higher sensing sensitivity was attributed to a thinner diameter of optical fiber in the range of 0.20–1.27 μm (1.27–4 μm) and a longer detection wavelength. When the diameter distributed in 2.3–3.91 μm, and the detection wavelength was 1550–1600 nm, the sensitivity reached 5.54–22.81 pm/°C. In 2018, Ahmad [28] et al. demonstrated a MKR temperature sensor without any packaging process. The temperature sensitivity of 14.5 pm/°C was experimentally obtained with good linearity during 27–95 °C. MKR temperature sensors can also be realized by connecting or combining other optical fiber structures. In 2012, Wu [29] et al. proposed a cascaded MKRs with two knot resonators having the similar diameter of ~500 μm. The differential measurement method was used to simultaneously measure temperature and other parameters to avoid the crosstalk sensitive property of muti-parameters.

In some cases, the temperature sensitive property should be restrained, in which another type of material with an inhibitory effect was used to guarantee the stability of MKR. For example, in practical applications, the magnetic field sensors are susceptible to the fluctuation of ambient temperature, which plays an important role in developing the MKR based magnetic field sensors. In 2014, an MKR temperature-insensitive magnetic field sensor with a cladding layer of ferrofluid (FF) was proposed [30]. The magnetic sensor has been prepared and proved experimentally with the sensitivity of 0.17 pm/°C. When the diameter of MNF was limited in a certain range, the thermal effect can be effectively suppressed. The applications of the MKRs are flexible by connecting in series, or combining with other kinds of fiber structures. The composite structures can improve the sensing performance, however, the operation and detuning is complex, the stability is poor without any packaging and the service life is limited. To pave the ways of the MKR temperature sensors to the commercial applications, the packaging techniques will be the most challenge work for the future research.

Wu et al. compared the temperature sensing performance of the silica and poly(methyl methacrylate) (PMMA) MKRs [31]. In this work, MKR was sandwich packaged by two magnesium difluoride (MgF_2) sheets, as

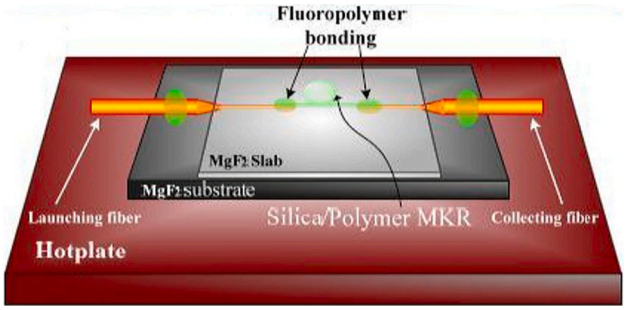

Fig. 2. Schematic diagram of MKR temperature sensing structure [31].

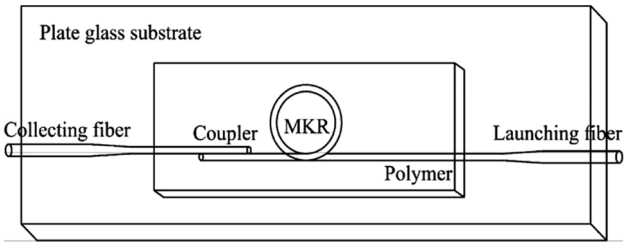

Fig. 3. Schematic diagram of MKR temperature sensor consisting of two single-mode optical fibers [32].

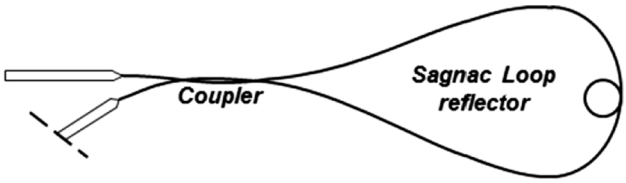

Fig. 4. Schematic diagram of MKR [33].

indicated in Fig. 2. The refractive index of either PMMA or MgF_2 is less than that of silica to avoid the light leakage. MKR structures could be fabricated by either coupling two MNFs or knotting one fiber. However, the corresponding fabrication process for this kind of MKR structure was complicated and rarely applied in the following years. The subsequent trials and iterations supported that the latter method would be better to obtain a fixable MKR structure.

As early as 2009, Zeng [32] et al. coated glass panels with the polymer film (EFIRON-UVF-PC373) by photolithography, the corresponding structure is illustrated in Fig. 3. They assembled MKR by manipulating the free end of MNF and placed it on the polymer substrate. The ring diameter was ~55 μm. To eliminate the environmental influence and enhance the stability of the MKR structure, a second layer of polymer was coated. The experimental sensitivity was 0.27 nm/°C for increasing temperature from 25 °C to 140 °C and −0.28 nm/°C during cooling process from 135 °C to 25 °C. A simple and efficient manufacturing method of MKR is proposed in this article and is widely used in many works reported later. Although the low refractive index polymer material is introduced, it is only used as a packaging medium to protect the MKR structure and improve the stability of the sensing probe. The sensitivity enhancement characteristics of the packaging materials have not been thoroughly studied, which will greatly improve the sensing performance of the MKR sensor probe.

In 2012, Lim et al. inserted a MKR structure in a Sagnac ring reflector to explore a temperature sensor [33], as shown in Fig. 4. Sagnac loop reflectors collect signals through the incident path, making the signal path in the device more efficient in terms of cost and response time. In the experiment, except for the junction resonator MKR, other parts were embedded in low refractive index PTFE for temperature measurement. The linear working range was experimentally demonstrated from 30 to 130 °C with a sensitivity of 20.6 pm/°C. It is lower than those reported in the works of Xu Zeng [31] and Yu Wu [32]. Because the MKR sensing part is directly placed on the glass plate, instead of being embedded in PTFE as other parts, or other processing, the low thermal conductivity of glass plate and MKR failed to contribute to a high sensitivity in the heating process. Moreover, the introduced MKR structure has not been fully applied, and the interference wavelength of the Sagnac interferometer is changed only by the change of its length or equivalent refractive index.

Some temperature-sensitive materials with low refractive index were introduced to coat or package the silicon MKR to maintain the structures, improve its lifetime, meet the resonance conditions, and avoid environmental pollution. Polydimethylsiloxane (PDMS) has a much larger thermal expansion coefficient and the thermal optical coefficient compared with that of silicon. In 2014, Yang et al. covered PDMS film on MKR to measure seawater temperature [34]. The relationship between sensitivity and detection wavelength, resonant ring diameter and fiber diameter has been studied. In this work, the temperature sensitivity of 0.197 nm/°C has been demonstrated around 1550 nm when the thickness of the PDMS film was 5 μm. With the increase of temperature, the morphology of MKR (depending on the thermal expansion of materials) and the refractive index of MNF (caused by the thermo-optical effects) become different to change the optical phase and result in the red-shift of the resonance wavelength. During the temperature sensing process, the refractive index of PDMS changes with the temperature and results in the different transmission mode. Therefore, the effective refractive index, phase and propagation constant are changed accordingly. Furthermore, the thermal expansion of PDMS will change the ring length of the MKR. Furthermore, as a temperature sensitive material, PDMS has high thermal stability up to 250 °C due to its unique molecular network structure [35]. PDMS is a high transparency and high flexibility film with the low refractive index of 1.406.

In 2018, Wang et al. fabricated MNF with a diameter of 3 μm and a tapered area in the length of 3 cm based on the standard single-mode optical fibers and flame brushing technology [36]. The MNF was directly knotted and fixed on the MgF_2 platform. A single-layer of graphene was peeled off from copper foil and transferred onto PDMS film. Where, two PDMS-graphene films (PGF) packaged the MKR as a sandwich structure. Two free ends of MKR were fixed on the substrate with high temperature resistant tapes. The MKR structure was lighted by 632.8 nm light and tightly wrapped by two pieces of PGF to form a compact and stable sandwich structure with a diameter of 185 μm. Graphene has a unique atomic orientation and gap-free structure, good electronic and photonic characteristics [37-39]. In particular, because of the high electron mobility and single layer nanostructure, its light absorption is easily affected by temperature [40]. MNF are in close contact under the action of PDMS to improve the sensitivity in this experiment.

To protect and support graphene film, PDMS was used making the MNF contacting closely with graphene and improving the stability of the device. Combining the advantages of two thermal-sensitive materials, a temperature sensor with a better performance has been obtained. Here, PDMS has a smaller thermal conductivity compared to graphene, which is the main factor affecting the response rate of PDMS, and can be calculated as [41]:

$$\tau = c\rho i^2/2h \tag{8}$$

where c is the specific heat, ρ is density, i is thickness, and h is thermal conductivity of PDMS, respectively. For PDMS films used in above work, $c = 1.38\text{j g}^{-1}\text{ K}^{-1}$, $\rho = 1.05\text{ g cm}^{-3}$, $i = 0.165$ mm, $h = 0.17\text{ W}^{-1}$ ($\text{m}^{-1}\text{ K}^{-1}$), resulting in a response time of 56 ms. It is slightly larger than the response time of the polymer MKR reported earlier [42]. The total reflection formed at the interface of MNF and PDMS can reduce the optical transmission loss. The 10-folds higher thermal coefficient of PDMS compared to MNF can significantly improve the temperature

response [13].

By comparing above methods, it is known that the MKR structure can be effectively protected to improve its stability and resistant to the environmental fluctuation by either covering materials or standing on materials coated MgF_2 or glass sheets. Although the introduced indirect relationship will exert some errors on the sensing performance when a new cover layer with low refractive index is coated on the MKR structure, the corresponding influence is always within an allowable range for the experimental conditions.

3.2. Humidity sensing applications

Generally, the humidity sensors can be improved by optimizing the fiber materials and coatings, such as the MKR humidity sensor made of polyacrylamide (PAM) by Wang [43] et al. in 2011. Where, the PAM absorbed water molecules and expanded, and the resonance peak exhibited an obvious shift in ~120 ms. During 5–71 %RH, the sensitivity up to 490 pm/%RH was obtained. To eliminate other influencing factors, Wu [44] et al. fabricated the miniature MKR humidity sensors directly from pure silica/PMMA without coating moisture materials. The humidity sensitivities of silicon and PMMA MKR sensor are ~1.2 pm/% RH and ~88 pm/10 %RH in linear ranges of 15–60 %RH and 17–95 % RH, respectively. Different fiber materials have been demonstrated according to the measuring environment and appropriate response time. In addition, the coating layers play an important role in humidity sensors. Unlike temperature-sensitive materials, humidity-sensitive materials must be in frequent contact with water molecules. On the one hand, its microporous structure automatically adsorbs water molecules in the air to change the equivalent refractive index of the film; on the other hand, the recovery time and stability of the water-containing film are poor, which will become a huge obstacle to its practical application. Porous semiconductor and polymer materials are the most commonly used humidity-sensitive materials, and have been widely used in the development of miniature MKR humidity sensors in recent years.

The humidity adsorption rate of TiO_2 is high due to its porous structure, which enables it to easily collect the water vapor molecules at room temperature. Faruki et al. compared the humidity sensing performance of the bare MKR with that of the titanium dioxide (TiO_2) nanoparticles coated MKR in 2016 [45]. The sensitivity has been obviously improved from 1.3 pm/%RH to 2.5 pm/%RH by elaborating the TiO_2 nanoparticles. Nanoparticles provide a large specific surface area and improve the ability to collect trace amounts of water molecules. The similarly work was reported by Azzuhri et al. in 2018, where the bare and the graphene oxide (GO) layer functioned MKRs were compared [46]. The two-dimensional structure and large surface area of GO make it is possible to highly sense the surrounding environment. Experimental comparisons reveal that the introduction of selective coatings can effectively improve the performance of humidity sensors, promoting many potential sensing applications for MKR sensors, especially for measuring the related parameters of climate and atmospheric.

Nafion is a promising coating material for the humidity sensors working in water environment because of its high hydrophilicity, thermal stability, high conductivity, mechanical toughness, low refractive index and high adhesion to silica. The MKR humidity sensor mentioned above has been tested in an air environment. In 2014, Gouveia et al. used Nafion as a coating layer of MKR to conduct an embedded silica MKR humidity sensor and studied its humidity sensing properties in an aqueous environment [47]. Two perfect linear ranges were obtained in the experiment. When humidity increase and decrease during 30 %RH and 75 %RH, two sensitivities of ~0.11 nm/%RH and ~0.08 nm/%RH were obtained in a low humidity region of 30–45 %RH, respectively; two sensitivities of ~0.29 nm/%RH and ~ 0.26 nm/%RH were obtained in a high humidity region of 40–75 %RH, respectively. During the characterization process, a hysteresis of ~1.9 nm was also observed. Both different sensitivities and hysteresis are dependent on the material properties of Nafion, such as its dilation hysteresis and abnormal water absorbency under the critical conditions of high dry and humidity environments [48]. Shin et al. used polyvinyl alcohol (PVA) elaborated MKR to detect the relative humidity [49]. Where the spatial frequency of four different modes were traced with the increase of humidity, and the highest sensitivity of $-0.87\ \mu m^{-1}$/%RH was realized in the range of 20–80 %RH for the highest order mode.

For sensitive materials, the hydrophilic materials can significantly deform the morphology of fiber structures by absorbing water molecules. The cost and lifetime of materials should be taken into account according to the working environments. To choose the packaging or coating film materials, besides the refractive index difference and hydrophilicity, the excellent compatibility between selected materials and substrates will effectively enhance the stability and service life of the humidity sensors. Furthermore, some special fibers or novel techniques are desired to enrich the research of MKR humidity sensors [50,51].

3.3. Refractive index sensing applications

The optical fiber sensors work based on the relationship between its equivalent refractive index and the power, phase and transmission time of the optical signal. The refractive index sensor has the basic functions of an optical fiber sensor, and be developed into a variety of multifunctional physical and biochemical sensors through optical fiber surface functionalization and sensitive material modification. MKR refractive index sensor is a very typical resonant cavity fiber device. In 2011, Pal et al. used multimode optical fiber to construct the MKR structure [52]. The middle part was corroded with hydrofluoric acid instead of the traditional melt-heating and taper-stretching process. The chemical etching method exposes the fiber core to generate an optical evanescent field, where the fiber diameter is precisely controlled by the etching time. The manufacturing cost of this process is low, and it can be flexibly adjusted according to the types and distribution characteristics of impurity particles in the optical fiber. However, the surface quality of this type of fiber is poorer than that of the hot-melt fiber, which results in light signal scattering. In 2014, Li proposed a dip-coating technique to fabricate a long-term stable MKR refractive index sensor [53], which can prevent the mechanical and optical degradation while maintaining a strong evanescent wave. The dip-coating process is divided into three steps. Firstly, MKR was completely wetted by immersing in Teflon solution; secondly, the wet MKR was dried for 10 min at 50 °C; finally, the film with uniform thickness was coated on the MNF surface after the solvent evaporated. The film thickness can be manipulated by the lifting speed due to the liquid viscous force on the MNF [54]. The resonance wavelength performed linear function of the surrounding environment, in which a lowest detection limit of 2×10^{-4} was obtained.

The MKR refractive index sensor has various structures. In 2014, Yu et al. assembled MKR with a very fine optical fiber (1.3 μm in diameter), and studied its sensing performance for determining analyte concentration from 0.6% to 1.2% [55]. The strong optical evanescent field is extremely sensitive to changes in refractive index near the optical fiber. It is tied around the optical fiber and can be efficiently coupled into the MKR structure after completing the information interaction with the outside environment. It also provides the possibility of integration of MKR structure or fiber structure with two-dimensional planar waveguide. In 2016, Gomes made a large-scale MKR with a diameter of several millimeters for sensing refractive index change [56]. A sensitivity reached 642 ± 29 nm/RIU and the resolution was 0.009 RIU in a working range of 1.3735–1.428. The manufacturing difficulty of large-size MKR is greatly reduced, which has become an important direction for the practical application of the device. Xu et al. verified the refractive index sensor with Vernier effect based on cascaded MKRs [57,58]. They utilized both the high-ratio evanescent field of MNF and the spectral amplification function of the Vernier effect to improve the sensitivity and detection resolution. The compact cascaded MKRs was prepared using the knot-assembled method [59]. By introducing the Lorentz transmission spectrum fitting algorithm, they experimentally

determined the lowest measuring value of 1.533×10^{-7} RIU. The cascade structure greatly improves the sensitivity of the MKR sensor, but the manufacturing process is complicated and the technical difficulty is relatively high. Combining the flexible micro-manipulation of the optical fiber and the precise design of the two-dimensional micro-disk structure, the repeatability and structural stability of the cascaded MKR structure can be improved. The cascade structure can also be used to expand the function of the optical fiber sensor and realize multi-parameter sensing. In 2017, Gomes and Frazo demonstrated the temperature and refractive index sensing performance of the compact composite structure consisting of MKR and an abrupt taper-based Mach-Zehnder interferometer [60]. Two spectral characteristic components were presented and responded to each measurement parameter. The cascade structure based on the same or different fiber structure makes full use of the optical sensing characteristics of the fiber, and can be used to design multi-parameter sensors and multi-point distributed sensors.

The structure of the MKR refractive index sensor is flexible. In the manufacturing method, the single MKR is easiest and most convenient for either the required experimental equipment or operation, but its sensitivity is relatively low. The double MKRs or other composite structures containing MKR has effectively improved the sensitivity and realized the muti-parameter measurement. It is necessary to choose suitable structures under the specific conditions.

3.4. Current sensing applications

Optical fiber current sensor has the potential applications in various industrial areas because of the unique characteristics, such as the miniature scale, anti-electromagnetic interference and excellent insulation performance. Optical fibers cannot be used for transmitting current, so MKR current sensors turns out with a relatively simple structure and mostly carried out by the assistance of metal and other conductive materials. In 2011, Lim et al. designed the current sensor by wrapping the copper wires around on the MKR structure [61]. The wavelength shift plays a linear relationship as a function of current square (A^2), and a sensitivity was achieved as 51.3 pm/A^2 for the developed device. Another current sensor consisting MKR and copper wire was proposed [62], two single mode optical fibers were used as input and output optical waveguides, respectively. The copper wire was firmly touched with the ring section of MKR. The MKR structure was heated by the flowing current, resulting in the resonance peak shift. This MKR current sensor is essentially a temperature sensor, which completes the energy conversion between temperature and current through a metal wire. This also inspired us that the same kind of optical fiber structure can realize the measurement of different parameters through the physical or chemical conversion between the measured parameters with the help of structural parameter optimization and smart materials. The current sensitivity was obtained as 90 pm/A^2 with a linear changing characteristic. Both methods are assisted by copper wires, but the relative position in the latter case caused a more obvious phase shift for the effective refractive index. The former wrapping structure is fragile.

In addition to the wire-assisted method, the magnetic fluid was coated on the MKR to exploring the current sensor [63]. Where, a MKR was covered by Teflon film, placed on an MgF_2 substrate and inserted into a small cavity filled with magnetic fluid. This MKR current sensor converts current changes into a magnetic field and acts on the magnetic fluid. It uses the magnetic field to modulate the refractive index of the magnetic fluid. Here, the direction of the electric field and magnetic field must be strictly controlled to achieve the most ideal sensing effect. The current sensing performance was verified by detecting a current signal with the 50 Hz sine wave and a pulse current signal with a rise time of 2.5 μs. The detection limit of 10 A was demonstrated with approximately linear relationship. Because the optical parameters of magnetic fluid won't be affected by the ambient temperature and stress, the reliability and accuracy of this sensor becomes better.

3.5. Other sensing applications

In recent years, the MKR based sensors have been widely used for detecting UV, hydrogen, alcohol, salinity, magnetic fields, pressure, acceleration and etc. The optimization ways are similar to the sensors mentioned above, for example, adding coatings, changing materials and alternating structures to improve the sensing performance.

3.6. Gas sensors

In 2015, Wu et al. adopted the palladium-coated MKR to determine the hydrogen concentration [64]. The recycling of resonance light in MKR can significantly accumulate hydrogen-palladium interaction and improve the detection sensitivity. In 2016, Yu et al. prepared a GO-deposited MKR for NH_3 and CO sensing [65]. When the concentration is less than 150 ppm, the sensitivity for detecting NH_3 is about 0.35 pm/ppm, and the sensitivity for detecting CO is ~0.17 pm/ppm. The corresponding sensitivities have been further increased by elaborating some special metal nanoparticles onto GO, such as palladium or platinum nanoparticles. Highly selective gas sensors rely on the molecular absorption spectrum and the selective absorption and catalytic properties of semiconductor materials. Fiber optic gas sensors based on various structures and new sensitive materials have huge application potential in narrow spaces, strong electromagnetic interference and toxic and harmful environments.

3.7. Magnetic sensors

Li et al. proposed the MKR magnetic sensor using a composite fiber structure filled with magnetic fluid [66]. The magnet fluid was filled into a sealed battery, in which the coupling region of a MKR was encapsulated by polymer. The magnetic sensitivity of 9.09 pm/mT was experimentally demonstrated with a regular curve. In 2017, Pu et al. compared the magnetic sensing performance of the MKR and Sagnac resonator [67]. In the same coupling region, the two resonators were encapsulated by magnetic fluid in capillary. The sensitivities of MKR and Sagnac resonator are 171.8 pm/Oe and 19.4 pm/Oe, respectively.

The MKR magnetic field sensor is realized based on the refractive index modulation characteristics of the magnetic fluid. The structure of the probe is complex and unstable due to the encapsulation of liquid sensitive materials and optical fiber coupling area. The introduction of hollow core fiber will help to develop more compact and stable magnetic field sensing probes.

3.8. Sensors for quantification and identification of analyte concentration

In 2014, Chiam et al. proposed a MKR alcohol detector. Where, the polyaniline (PANI) drop-coated on the MKR [68]. The wavelength shift in response to different concentrations of alcohol was recorded by analyzing the output spectra. The excellent repeatability was obtained. A simple MKR sensor for selectively detecting different alcohols was realized. Liao et al. studied the relationship between sensing sensitivity and optical fiber diameter or detection wavelength [69]. The results show that as the decrease of the diameter, and the increase of the detection wavelength (1500 nm to 1650 nm), the sensitivity increases, whose maximum value was demonstrated to be 21.18 pm/‰. This is due to the strong evanescent field effect of the sub-wavelength size optical waveguide. At the same time, label-free sensitive materials and functional modifications will also enrich the applications of MKR optical fiber sensors in the biological and chemical sensing fields.

3.9. Violet sensors

In 2013, Lim et al. proposed a PANI coated ultra-violet sensor based on MKR. During fabrication process, the PANI film was prepared on the MKR with the resonator diameter of 1 mm [70]. The resonance

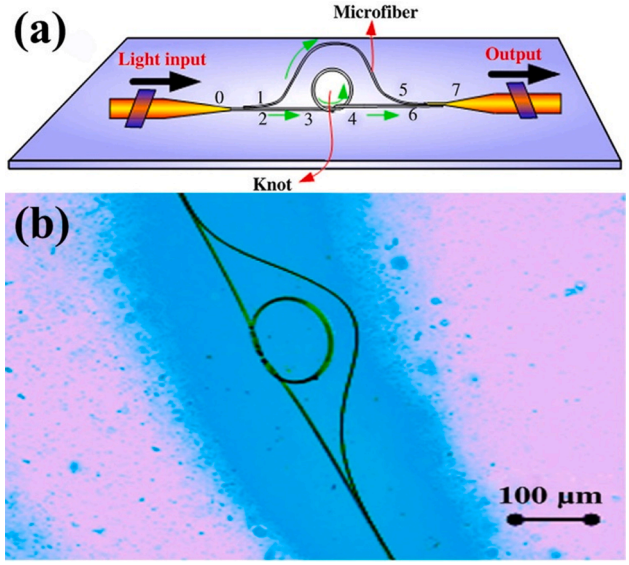

Fig. 5. (a) Schematic diagram and (b) micrograph of of MKR based Mach-Zehnder structure [74].

wavelength shifted with a linear relationship and the sensitivity of 6.61 nm/(W cm^{-2}) for the ultraviolet light intensity. Compared with the traditional ultraviolet detector, the detector has the advantages of anti-electromagnetic interference, small volume, good physical flexibility and simple manufacturing process. In 2015, Sulaiman et al. prepared a ytterbium-doped MKR and observed the fluorescence violet conversion luminescence for the first time [71]. Chen et al. accomplished a violet MKR sensors by coating its surface with tungsten disulfide nanosheets [72]. The sensitivity reached up to ~0.4 dB/mW, and the average response time is ~1.2 s. Functional polymer-based flexible optical fibers and ultra-fine optical fibers are easier to integrate into fabrics and other wearable devices, realizing real-time monitoring of optical environmental pollution and internal mechanical stress changes.

3.10. Mechanical sensors

In 2014, Wu et al. proposed and demonstrated a micro-optoelectronic system accelerometer based on MKR [73], which was firstly used for optical detection of the structural vibrations of micro-electromechanical system. The resonance wavelength depends on acceleration with a sensitivity of 29 pm/g. These MKR devices were also widely used in the field of communications. Fig. 5 illustrates a flexible integrated waveguide device, consisting a MKR based Mach-Zehnder structure, which was proposed by Chen in 2010 [74]. Its Q factor was significantly improved compared to that of the common Mach-Zehnder interferometer. This novel device could be optimized by selecting paths difference or coupling distance.

In 2017, Li et al. proposed a hybrid plasmon MKR to measure the weight [75]. The substrate surface of the device was functionalized with gold nanofilm and packaged in PDMS. The Q factor is greater than 47,000 and the weight sensitivity is 9.34 pm/kPa, which is higher than most conventional pressure sensors. The bending was determined by the variations of ring length and effective index of MKR structure [76]. The experimental sensitivity and theoretical resolution are 3.04 nm/m^{-1} and 3.29 × 10^{-3} m^{-1}, respectively.

3.11. Photonics devices and sensors

MKR are the promising candidate for developing the all-optical devices, such as modulators, polarizer, filter or sensors [77,78]. In 2015, Xu et al. theoretically and experimentally studied the slow-light characteristics of parallel MKRs [79]. When this resonator was launched by a 3.35 GHz pulse signal, a large group delay is obtained. This device has the promising potentials in optical storage, quantum communications and so on. The group delay MKR devices was also used for sensing relative humidity, as reported recently in Ref. [50].

Generally, the optical fiber material for preparing MKR is silica, because of its mature manufacturing process and low cost. Silica-MKR structure is modified with different sensitive materials to develop different kinds of sensor probes. Table 1 lists the different materials modified silica-MKR structure used to achieve the measurement of

Table 1
Sensing performance of silica-MKR sensors elaborated by different materials.

Elaborate materials	Measurement target	Sensitivity	Working range	Reference
EFIRON-UVF-PC373	Temperature	0.27 nm/°C	25–140 °C	[26]
PMMA	Temperature	~266 pm/°C	20–80 °C	[27]
PDMS	Temperature	0.197 nm/°C	Not given	[28]
PTFE	Temperature	20.6 pm/°C	30–130 °C	[29]
PDMS-Graphene Film	Temperature	0.544 dB/°C	30–60 °C	[30]
PDMS	Temperature	24.6 nm/°C	32–45 °C	[38]
Glycerin Liquids	Temperature	~-230 pm/°C	20–60 °C	[40]
PAM	Humidity	490 pm/%RH	5–71 %RH	[43]
TiO2 Nanoparticles	Humidity	2.5 pm/%RH	40–95 %RH	[45]
Graphene Oxide	Humidity	~10 pm/%RH	0–80 %RH	[46]
Nafion	Humidity	~0.3 nm/%RH	40–75 %RH	[47]
PVA	Humidity	~0.87 nm/%RH	20–80 %RH	[49]
PVA	Humidity	−0.99 μm^{-1}/% RH	35–80 %RH	[50]
Teflon	Refractive index	~31 nm/RIU	1.3322–1.3412	[53]
PTT	Refractive index	95.5 nm/RIU	1.39–1.41	[55]
Copper Wire (wind)	Current	51.3 pm/A^2	0–2 A	[61]
Copper Wire (near)	Current	90 pm/A^2	0–2 A	[62]
Magnetic Fluid	Current	~2.25 mV/A	0–2000 A	[63]
Pd Nanoparticles	Hydrogen	~4.4 nm/%	0–9.1%	[64]
Graphene Oxide	CO and NH_3	0.35 pm/ppm ~0.17 pm/ppm	0–400 ppm	[65]
Magnetic Fluid	Magnetic	9.09 pm/mT	0–22 mT	[66]
Magnetic Fluid	Magnetic	171.8 pm/Oe	0–240 Oe	[67]
PAni	Alcohol	21.18 pm/‰	0–50%	[68]
PAni	Ultra-violet	6.61 nm/(W cm^{-2})	10–22.5 mW/cm^2	[70]
WS_2 Nanosheets	Ultra-violet	~0.4 dB/mW	0–23.6 mW	[72]
Epotek OG134	Accelerate	o.o29 nm/g	0–25 g	[73]
Gold Film + PDMS	Weight	9.34 pm/kPa	0–42 kPa	[75]
Glue + Steel Blades	Bending	3.04 nm/m^{-1}	0–0.15 m^{-1}	[76]

temperature, humidity, refractive index, current and other parameters. These materials are mostly polymers, which can effectively improve the flexibility, sensitivity and corrosion resistance of optical fiber sensor probe.

4. Forecast and prospect

The MKR fiber structure has high stability and low cost compared to other commonly used fiber structures. However, the coupling area of the MKR must be carefully packaged to ensure stable transmission of optical signals. Corresponding encapsulation materials are mainly polymer materials, and doped with new functional nanomaterials to improve the sensitivity and selectivity of the sensor device. With the ultra-high specific surface area of nanoparticles, the sensitivity of the sensor has been effectively improved; sandwich packaging MKR based on two-dimensional materials is easier to integrate into wearable devices; transitional sensitive materials effectively expand the application field of sensors by converting the different parameters, such as the current sensors mentioned in the manuscript; s The cascade of MKR and other optical fiber structures provides a reference for the development of multi-parameter array sensors; the emergence of a variety of novel optical fibers will also greatly optimize the structure and sensing performance of MKR sensors.

5. Conclusions

In summary, due to the high sensitivity, high resolution, and rapid response, MKR sensors have achieved a great progress in both theory and experiment in recent years. More breakthroughs will turn out in the future. Although many experimental models have been demonstrated in the past ten years, the shortcomings of the MKR cannot be overcome completely. MKR similar structures are fragile because of the thin diameter of optical fiber. The preservation of MNFs, the surface encapsulation of MKRs, the stability and the protection of fusion knots will exert an impact on the practical sensing. In order to fabricate MKRs with higher sensitivity and better practicability, the future research should be focused on optimizing the fabrication process, enhancing structural stability, adopting the proper sensitive materials and packaging forms. For fabricating the MKR sensors with higher stability or repeatability and pave their way to future applications, more stable and uniform MNF is needed to prepare by the novel techniques.

CRediT authorship contribution statement

Hongtao Dang: Conceptualization, Writing - original draft. **Mingshu Chen:** Data curation, Visualization, Data curation, Visualization. **Jin Li:** Supervision, Funding acquisition. **Wei Liu:** Writing - review & editing.

Declaration of Competing Interest

The authors declare that they have no known competing financial interests or personal relationships that could have appeared to influence the work reported in this paper.

Acknowledgement

This work was supported by the National Key R&D Program of China (2019YFB2006001), Fundamental Research Funds for Central Universities (N2004007) and Xi'an Science and Technology Plan (2020KJRC0133).

References

[1] Y. Wu, L. Jia, T.H. Zhang, Y.J. Rao, Y. Gong, Microscopic multi-point temperature sensing based on microfiber double-knot resonators, Opt. Commun. 285 (2012) 2218–2222.
[2] S. Wang, T. Liu, X. Wang, Y. Liao, J. Wang, J. Wen, Hybrid structure Mach-Zehnder interferometer based on silica and fluorinated polyimide microfibers for temperature or salinity sensing in seawater, Measurement 135 (2019) 527–536.
[3] J. Li, H. Yan, H.T. Dang, F.L. Meng, Structure design and application of hollow core microstructured optical fiber gas sensor: A review, Opt. Laser Technol. 135 (2021) 106658.
[4] Y. Liu, X. Li, Y.N. Zhang, Y. Zhao, Fiber-optic sensors based on Vernier effect, Measurement 167 (2021) 108451.
[5] M. Yasin, N. Irawati, S.W. Harun, F. Ahmad, M. Khasanah, Sodium nitrate (NaNO3) sensor based on graphene coated microfiber, Measurement 146 (2019) 208–214.
[6] Z.Y. Yuan, E.C. Han, F.L. Meng, K.Y. Zuo, Detection and identification of volatile organic compounds based on temperature-modulated ZnO sensors, IEEE Trans. Instrum. Meas. 69 (2020) 4533–4544.
[7] C. Wang, W. Jin, W. Jin, J. Ju, J. Ma, H.L. Ho, Evanescent-field photonic microcells and their applications in sensing, Measurement 79 (2016) 172–181.
[8] F. Vial, K. Gadonna, B. Debord, F. Delahaye, F. Amrani, O. Leroy, F. Gérôme, F. Benabid, Generation of surface-wave microwave microplasmas in hollow-core photonic crystal fiber based on a split-ring resonator, Opt. Lett. 41 (2016) 2286–2289.
[9] B. Bhola, H.C. Song, H. Tazawa, W.H. Steier, Polymer microresonator strain sensors, IEEE Photonics Technol. Lett. 17 (2005) 867–869.
[10] M. Belal, Z. Song, Y. Jung, G. Brambilla, T.P. Newson, Optical fiber microwire current sensor, Opt. Lett. 35 (2010) 3045–3047.
[11] P.R. Watekar, S. Ju, S.A. Kim, S. Jeong, Y. Kim, W.T. Han, Development of a highly sensitive compact sized optical fiber current sensor, Opt. Express 18 (2010) 17096–17105.
[12] J. Li, C.X. Liu, H.F. Hu, Q. Wang, Y. Zhao, Ag micro-spheres doped silica fiber used as a miniature refractive index sensor, Sensor Actuat B-Chem 223 (2016) 241–245.
[13] J. Li, Z.B. Li, J.T. Yang, Y. Zhang, C.Q. Ren, High sensitivity temperature probe based on elliptical microfiber knot ring, Results Phys. 16 (2020) 102953.
[14] L. Shi, Y. Xu, W. Tan, X. Chen, Simulation of optical microfiber loop resonators for ambient refractive index sensing, Sensors 7 (2007) 689–696.
[15] W.Q. Qiu, J.J. Zhou, J.H. Yu, Y. Xiao, H.H. Lu, H.Y. Guan, Y.C. Zhong, J. Zhang, Z. Chen, Theoretical analysis of polarization-coupled mode splitting in a single microfiber knot-ring resonator, Opt. Eng. 55 (2016) 066108.
[16] M.S. Yoon, Y.G. Han, Highly sensitive current sensor based on an optical microfiber loop resonator incorporating low index polymer, Int. Conf. Opt. Fibre Sens. Int. Soc. Opt. Photon. 23 (2014) 86–91.
[17] X. Xie, J. Li, L.P. Sun, X. Shen, L. Jin, B.O. Guan, A high-sensitivity current sensor utilizing CrNi wire and microfiber coils, Sensors 14 (2014) 8423–8429.
[18] L.M. Tong, R.R. Gattass, J.B. Ashcom, S. He, J.Y. Lou, M.Y. Shen, I. Maxwell, E. Mazur, Subwavelength-diameter silica wires for low-loss optical wave guiding, Nature 426 (2003) 816–819.
[19] Y. Semenova, L. Bo, S. Mathews, P.F. Wang, Q. Wu, G. Farrell, Spectral tuning of a microfiber coupler with a liquid crystal overlay, Int. Conf. Opt. Fiber Sens. 22 (2012) 8421–8424.
[20] Y.P. Xu, L.Y. Ren, C.J. Ma, J. Liang, Theoretical study on slow light in different structures of optical microfiber knot resonators, Optik-Int. J. Light Electron. Opt. 125 (2014) 2856–2861.
[21] K. Morishita, T. Yamaguchi, Wavelength tunability and polarization characteristics of twisted polarization beamsplitting single-mode fiber couplers, J. Lightwave Technol. 19 (2001) 732–738.
[22] L.F. Stokes, M. Chodorow, H.J. Shaw, All-single-mode fiber resonator, Opt. Lett. 7 (1982) 288–290.
[23] C.K. Madsen, G. Lenz, Optical all-pass filters for phase response design with applications for dispersion compensation, IEEE Photon. 10 (1998) 994–996.
[24] G.T. Paloczi, Y. Huang, A. Yariv, Free-standing all-polymer microring resonator optical filter, Electronics 39 (2003) 1650–1651.
[25] M. Sumetsky, Y. Dulashko, J.M. Fini, A. Hale, D.J. Digiovanni, The microfiber loop resonator: theory, experiment, and application, J. Lightwave Technol. 24 (2006) 242–250.
[26] X. Li, H. Ding, Temperature insensitive magnetic field sensor based on ferrofluid clad microfiber resonator, Photon. Technol. Lett. IEEE 26 (2014) 2426–2429.
[27] X. Li, H. Ding, Investigation of the thermal properties of optical microfiber knot resonators, Instrum. Sci. Technol. 41 (2013) 224–235.
[28] H. Yang, S. Wang, X. Wang, J. Wang, Y. Liao, Temperature sensing in seawater based on microfiber knot resonator, Sensors 14 (2014) 18515–18525.
[29] H. Ahmad, A.S. Zulkhairi, S.R. Azzuhri, Temperature sensor and fiber laser based on optical microfiber knot resonator, Optik: Int. J. Light Electron Opt. 154 (2018) 294–302.
[30] Y. Wu, Y. Chen, Y. Rao, T. Zhang, Y. Gong, Microscopic multi-point temperature sensing based on microfiber double-knot resonators, Opt. Commun. 285 (2012) 2218–2222.
[31] Y. Wu, Y.J. Rao, Y.H. Chen, Miniature fiber-optic temperature sensors based on silica/polymer microfiber knot resonators, Opt. Express 17 (2009) 18142–18147.
[32] X. Zeng, Y. Wu, C. Hou, J. Bai, G. Yang, A temperature sensor based on optical microfiber knot resonator, Opt. Commun. 282 (2009) 3817–3819.
[33] K.S. Lim, I. Aryanfar, W.Y. Chong, Y.K. Cheong, S.W. Harun, H. Ahmad, Integrated microfibre device for refractive index and temperature sensing, Sensors 12 (2012) 11782–11789.

[34] H. Yang, S. Wang, K. Mao, G. Li, J. Wang, Numerical calculation of seawater temperature sensing based on polydimethylsiloxane-coated microfiber knot resonator, Opt. Photon. J. 4 (2014) 91–97.
[35] Y. Aoki, K. Yoshioka, Preparation and characterization of highly heat-resistant organic–inorganic hybrid materials made from two-component polydimethylsiloxane, Mol. Cryst. Liq. Cryst. 597 (2014) 59–64.
[36] M.Q. Wang, D. Li, R.D. Wang, J. Zhu, Z. Ren, PDMS-assisted graphene microfiber ring resonator for temperature sensor, Opt. Quant. Electron. 50 (2018) 132–134.
[37] Q. Cheng, J. Tang, J. Ma, H. Zhang, N. Shinya, L.C. Qin, Graphene and carbon nanotube composite electrodes for supercapacitors with ultra-high energy density, PCCP 13 (2011) 17615–17624.
[38] X.H. Sun, Q.Z. Sun, W.H. Jia, Z.L. Xu, J.H. Wo, D. Liu, Z. Lin, Graphene coated microfiber for temperature sensor, Fiber-Based Technol. Appl. (2014) FF4B.3.
[39] E. Pallecchi, F. Lafont, V. Cavaliere, F. Schopfer, D. Mailly, W. Poirier, A. Ouerghi, High electron mobility in epitaxial graphene on 4H-SiC(0001) via post-growth annealing under hydrogen, Sci. Rep. 4 (2014) 4558–4564.
[40] B.C. Yao, Y. Wu, A.Q. Zhang, Y.J. Rao, Z.G. Wang, Y. Cheng, Y. Gong, W.L. Zhang, Y.F. Chen, K.S. Chiang, Graphene enhanced evanescent field in microfiber multimode interferometer for highly sensitive gas sensing, Opt. Express 22 (2014) 28154–28162.
[41] P. Yi, R.A. Awang, W.S. Rowe, K. Kalantar-zadeh, K. Khoshmanesh, PDMS nanocomposites for heat transfer enhancement in microfluidic platforms, Lab Chip 14 (2014) 3419–3426.
[42] R.B. Smith, Analytic solutions for linearly tapered directional couplers, J. Opt. Soc. Am. 66 (1976) 882–892.
[43] P. Wang, F.X. Gu, L. Zhang, L.M. Tong, Polymer microfiber rings for high-sensitivity optical humidity sensing, Appl. Opt. 50 (2011) G7–G10.
[44] Y. Wu, T.H. Zhang, Y.J. Rao, Y. Gong, Miniature interferometric humidity sensors based on silica/polymer microfiber knot resonators, Sens. Actuators, B 155 (2011) 258–263.
[45] M.J. Faruki, A. Razak, S.R. Azzuhri, M.T. Rahman, M.R.K. Soltanian, G. Brambilla, B.M. AzizurRahman, K.T.V. Grattan, R.D.L. Rue, H. Ahmad, Effect of titanium dioxide (TiO2) nanoparticle coating on the detection performance of microfiber knot resonator sensors for relative humidity measurement, Mater. Exp. 6 (6) (2016) 501–508.
[46] S.R. Azzuhri, I.S. Amiri, A.S. Zulkhairi, M.A. MSalim, M.Z.A. Razak, M. F. Khyasudeen, H. Ahmad, R. Zakaria, P. Yupapin, Application of graphene oxide based microfiber-knot resonator for relative humidity sensing, Res. Phys. 9 (2018) 1572–1577.
[47] M.A. Gouveia, P.E.S. Pellegrini, J.S. DosSantos, I.M. Raimundo, C.M.B. Cordeiro, Analysis of immersed silica optical microfiber knot resonator and its application as a moisture sensor, Appl. Opt. 53 (2014) 7454–7461.
[48] K.S. Lim, A.A. Jasim, S.S.A. Damanhuri, S.W. Harun, B.M. Rahman, H. Ahmad, Resonance condition of a microfiber knot resonator immersed in liquids, Appl. Opt. 50 (2011) 5912–5916.
[49] J.C. Shin, M.S. Yoon, Y.G. Han, Relative humidity sensor based on an optical microfiber knot resonator with a polyvinyl alcohol overlay, J. Lightwave Technol. 34 (2016) 4511–4515.
[50] A.D.D. Le, Y.G. Han, Relative humidity sensor based on a few-mode microfiber knot resonator by mitigating the group index difference of a few-mode microfiber, J. Lightwave Technol. 36 (2018) 904–909.
[51] Y.P. Liao, J. Wang, S.S. Wang, H.J. Yang, X. Wang, Spectral characteristics of the microfiber MZ interferometer with a knot resonator, Opt. Commun. 389 (2017) 253–257.
[52] S.S. Pal, S.K. Mondal, U. Tiwari, P.V. Swamy, M. Kumar, N. Singh, P.P. Bajpai, P. Kapur, Etched multimode microfiber knot-type loop interferometer refractive index sensor, Rev. Sci. Instrum. 82 (2011) 816–819.
[53] X.L. Li, H. Ding, A stable evanescent field-based microfiber knot resonator refractive index sensor, IEEE Photon. Technol. Lett. 26 (2014) 1625–1628.
[54] D. Grosso, How to exploit the full potential of the dip-coating process to better control film formation, J. Mater. Chem. 21 (2011) 17033–17038.
[55] H.Q. Yu, L. Xiong, Z. Chen, Q. Li, X. Yi, Y. Ding, F. Wang, H. Lv, Y.M. Ding, Solution concentration and refractive index sensing based on polymer microfiber knot resonator, Appl. Phys Express 7 (2014) 022501.
[56] A.D. Gomes, O. Frazão, Mach-Zehnder based on large knot fiber resonator for refractive index measurement, IEEE Photon. Technol. Lett. 28 (2016) 1279–1281.
[57] Z. Xu, Q. Sun, B. Li, Y. Luo, W. Lu, D. Liu, P.P. Shum, L. Zhang, Highly sensitive refractive index sensor based on cascaded microfiber knots with Vernier effect, Opt. Express 23 (2015) 6662–6672.
[58] Z.L. Xu, Y.Y. Luo, D.M. Liu, P.P. Shum, Q.Z. Sun, Sensitivity-controllable refractive index sensor based on reflective θ-shaped microfiber resonator cooperated with Vernier effect, Sci. Rep. 7 (2017) 9620.
[59] X.S. Jiang, Q. Yang, G. Vienne, Y.H. Li, L.M. Tong, J.J. Zhang, L.L. Hu, Demonstration of microfiber knot laser, Appl. Phys. Lett. 89 (2006) 839.
[60] A.D. Gomes, O. Frazão, Microfiber knot with taper interferometer for temperature and refractive index discrimination, IEEE Photon. Technol. Lett. 99 (2017) 1517–1520.
[61] K.S. Lim, S.W. Harun, S.S.A. Damanhuri, A.A. Jasim, C.K. Tio, H. Ahmad, Current sensor based on microfiber knot resonator, Sens. Actuators, A 167 (2011) 60–62.
[62] A. Sulaiman, S.W. Harun, J.M. Desa, H. Ahmad, Demonstration of DC current sensing through microfiber knot resonator, in: IEEE International Conference on Semiconductor Electronicsm vol. 2, IEEE, 2013, pp. 378–380.
[63] X.L. Li, F.X. Lv, Z.Y. Wu, H. Ding, An all-fiber current sensor based on magnetic fluid clad microfiber knot resonator, Proc. Int. Conf. Sens. Technol. 9 (2014) 418–421.
[64] X. Wu, F.X. Gu, H.P. Zeng, Palladium-coated silica microfiber knots for enhanced hydrogen sensing, IEEE Photon. Technol. Lett. 27 (2015) 1228–1231.
[65] C.B. Yu, Y. Wu, X.L. Liu, B.C. Yao, F. Fu, Y. Gong, Y.J. Rao, Y.F. Chen, Graphene oxide deposited microfiber knot resonator for gas sensing, Opt. Mater. Exp. 6 (2016) 727–733.
[66] X.L. Li, H. Ding, C.Y. Han, A novel magnetic field sensor based on the combination use of microfiber knot resonator and magnetic fluid, Int. Conf. Condit. Monit. Diagnosis 41 (2013) 111–113.
[67] S.L. Pu, L.M. Mao, T.J. Yao, J.F. Gu, M. Lahoubi, X.L. Zeng, Microfiber coupling structures for magnetic field sensing with enhanced sensitivity, IEEE Sens. J. 99 (2017) 5857–5861.
[68] Y.S. Chiam, K.S. Lim, S.W. Harun, S.N. Gan, S.W. Phang, Conducting polymer coated optical microfiber sensor for alcohol detection, Sens. Actuators, A 205 (2014) 58–62.
[69] Y.P. Liao, X. Wang, H.J. Yang, S.S. Wang, J. Wang, Resonant mode characteristics of microfiber knot-type ring resonator and its salinity sensing experiment, IEEE Photon. J. 7 (2015) 6802308.
[70] K.S. Lim, Y.S. Chiam, S.W. Phang, W.Y. Chong, C.H. Pua, A.Z. Zulkifli, I. Ganesan, S.W. Harun, H. Ahmad, A polyaniline-coated integrated microfiber resonator for UV detection, IEEE Sens. J. 13 (2013) 2020–2025.
[71] A. Sulaiman, S.W. Harun, Observation violet emission of microfiber knot resonator, Microwave Opt. Technol. Lett. 57 (2015) 2929–2931.
[72] G.W. Chen, Z.J. Zhang, X.L. Wang, H.G. Li, M.J. Jiang, H.Y. Guan, W.T. Qiu, H. H. Lu, J.L. Dong, W.G. Zhu, J.H. Yu, Y.C. Zhong, Y.H. Luo, J. Zhang, Z. Chen, Highly sensitive all-optical control of light in WS_2 coated microfiber knot resonator, Opt. Express 26 (2018) 27650–27658.
[73] Y. Wu, X. Zeng, Y.J. Rao, Y. Gong, C.L. Hou, G.G. Yang, MOEMS accelerometer based on microfiber knot resonator, IEEE Photon. Technol. Lett. 21 (2009) 1547–1549.
[74] Y.H. Chen, Y. Wu, Y.J. Rao, Q. Deng, Y. Gong, Hybrid Mach-Zehnder interferometer and knot resonator based on silica microfibers, Opt. Commun. 283 (2010) 2953–2956.
[75] J.H. Li, F. Xu, Y.P. Ruan, A hybrid plasmonic microfiber knot resonator and mechanical applications, Int. Conf. Opt. Commun. Netw. 20 (2017) 1–3.
[76] S. Dass, R. Jha, Square knot resonator-based compact bending sensor, IEEE Photon. Technol. Lett. 30 (2018) 1649–1652.
[77] Y.H. Meng, L. Deng, Z.L. Liu, H.F. Xiao, X.N. Guo, M.M. Liao, A.Q. Guo, T.H. Ying, Y.H. Tian, All-optical tunable microfiber knot resonator with graphene-assisted sandwich structure, Opt. Express 25 (2017) 18451–18461.
[78] J.H. Li, J.H. Chen, S.C. Yan, Y.P. Ruan, F. Xu, Y.Q. Lu, Versatile hybrid plasmonic microfiber knot resonator, Opt. Lett. 42 (2017) 3395–3398.
[79] Y.P. Xu, L.Y. Ren, J. Liang, C.J. Ma, Y.L. Wang, X.D. Kong, X. Lin, Slow light and fast light in microfiber double-knot resonator with a parallel structure, Appl. Opt. 34 (2015) 2724–2726.